



Mathematical Modelling & Numerical Analysis of
Passive Multimode Tuned Mass Damper
Mechanism for a Multiple Degree of Freedom
Structure

Afham Zulhusmi Bin Ahmad, Aminudin Abu, Lee Kee Quen,
Nor Azizi Othman and Faridah Che In

EasyChair preprints are intended for rapid
dissemination of research results and are
integrated with the rest of EasyChair.

November 27, 2020

Mathematical Modelling & Numerical Analysis of Passive Multimode Tuned Mass Damper Mechanism for a Multiple Degree of Freedom Structure

Afham Zulhusmi Ahmad ^{a, *}, Aminudin Abu ^a, Lee Kee Quen ^a, Nor A'zizi Othman ^a, Faridah Che In ^b

^a Malaysia-Japan International Institute of Technology (MJIT), Universiti Teknologi Malaysia, 54100 Kuala Lumpur, Malaysia

^b Politeknik Kuching Sarawak, KM 22 Jalan Matang, 93050 Kuching, Sarawak, Malaysia

*Corresponding author email: azulhusmi2@live.utm.my

Abstract

A single Tuned Mass Damper (TMD) can only suppress vibration of the assigned mode shape of a structure. For controlling multimode vibrations, Multiple Tuned Mass Damper (MTMD) is needed. In this study, mathematical modelling & numerical evaluation of the proposed MTMD as a vibration suppression mechanism is performed comprehensively by transforming structural model into an equivalent lumped mass-spring-dashpot system with consideration of Rayleigh damping hypotheses. The main structural model is designed as a linear time-invariant system and the equations of motions were derived using transfer function. The transfer function then further simplified in a state space representation to cater the analysis complexity. The time history & frequency response analysis of this study including the vibration control effect of attaching the various TMD arrangements to a three-story structure due to ground excitation input. A single TMD is first been designed to be tuned according to different mode shapes of uncontrolled primary structure. The influence of parameters such auxiliary mass ratio, optimum damping ratio, and optimum frequency ratio is identified numerically and the performance of structural control mechanism is analyzed for both single TMD and MTMD arrangement with additional base isolation system. The optimal placement of control devices is also justified using defined objective functions purposely to maximize system effectiveness and the robustness of the proposed mechanism in terms of the distribution of natural frequencies of seismic input. The result shows that the optimization of all TMD arrangements satisfied of reducing Root Means Square (RMS) acceleration of the top structural floor. The result show that by the attachment of TMD at all floors with additional base isolation system is capable of reducing significant amount

of top floor RMS displacement for a solid 94.5% for the first floor, 97.6% for the second floor, and 71.9% for the third floor.

Keywords: *Tuned Mass Damper, Base Isolation, Transfer Function, Frequency Response*

1. Introduction

Structural vibrations are caused due to various dynamic excitations. The most significant dynamic waves imposed to the structural systems are commonly carried by the nature such as wind, earthquake, and watercourse. In recent years, vast researchers dedicated their effort to extend existing findings on the improvement of structural vibration control devices and strategies, particularly to mitigate hazardous structural responses caused by these natural forces. This great motivation to design a robust control strategy is purposely to overcome the weaknesses of conventional design approach which traditionally, a structure only included with sufficient strength to withstand loads and limited capability to deform in a ductile manner. The limitations of the conventional method can be segregated into certain factors. The main factor is that structures dedicatedly rely on the small amount of material damping to dissipate vibration energy and it totally depends on their stiffness to resist horizontal loads.

Generally, there are various structural vibration control systems has been developed to mitigate structural responses [1]. One of those is passive control system. Passive control system is a promising vibration control technology for dissipation of seismic input via isolation and energy dissipation devices. The energy dissipation mechanism passive device is totally dependent on the relative movement of a structure which related to the local structural responses [2]. Nevertheless, the devices are inherently stable, do not require any external energy and require simple design to construct [3]. Within all devices under this classification, Tuned Mass Damper (TMD) has been extensively studied by researchers globally in terms of design development and optimization [4], [5], and [6].

2. Literature Review

A TMD system consists of an added mass with properly functioning spring and damping elements that provide frequency-dependent damping in a primary structure [7]. In practice, TMD dissipate substantive vibration of the main structure without any connection to the ground and inherently stable to work during major earthquake. The effectiveness of TMD can be determined by certain factors such its dynamic characteristics, damping stroke, and TMD mass ratio to the modal mass. In terms of operational mechanism, TMD will be tuned to the dominant natural frequencies of the primary structure to reduce unwanted vibration. However, this mechanism suffers certain drawbacks which related to the sensitivity against operating environmental changes due to structural deterioration which resulting to detuning. TMD ability is restricted to reduce vibration components which close to the tuned frequencies and significantly limited to narrow bandwidth [8], [9]. Therefore, it is inadequate for controlling structure under broadband excitation such earthquake.

To overcome current disadvantage, various methods and mechanism has been proposed to improve TMD performance reliability and robustness. One of a kind from those mechanisms is the implementation of Multiple Tuned Mass Damper (MTMD). In order to cover wider bandwidth, [10] used a total of seven TMD with different mass ratio to control buffeting problem faced by Yangpu Bridge. By adding near optimal amounts of TMD at various primary structure locations, [11] successfully dampened several of structural frequencies under proposed analysis and redesign scheme of MTMD mechanism. A study by [12] proved the effectiveness of MTMD to mitigate structural vibration modes. It was found that a two degree of freedom TMD is capable of reducing bending and torsional modes of a bridge deck simultaneously. In order to design an optimal operational condition, optimization of TMD design variables such as mass, period, and damping ratio are vital in the preliminary design stage to obtain structural steady state responses during ground excitation [13], [14], [15]. Nevertheless, it is found that there is still a loophole and room for design improvement. Most of researchers focusing on the TMD parameter optimization and limited conclusive findings on the performance and the feasibility of MTMD combination with other control method to produce a hybrid control mechanism. Therefore, there it is still a need to discover the potential of a new MTMD mechanism systematically for improving structural control performance.

3. Research Methodology

3.1 Structural-TMD Equation of Motion

The basic mathematical equation of motions modelling of a structure-TMD system is idealized using a three-story fixed base reinforced concrete structure equipped with a TMD. The structural behavior of the primary structural system can be represented as an idealized element such mass (m_i), damping (c_i), and stiffness (k_i) of the i^{th} story. The mass is assumed to be excited directly by external forces and assumed to be in equilibrium when applied forces is zero.

Energy is stored by the system in the mass and spring in the form of kinetic and potential energy. Energy enters the system through excitation and dissipated through damping. The TMD parameters represents as mass of the auxiliary (m_d), damping coefficient of the auxiliary system (c_d), and stiffness of the auxiliary system (k_d). The equations of motion of the coupled system is given an external excitation (P_0) which resulted relative displacement between the primary structure and the TMD (u_i). Considering free body diagram of multiple structural masses by applying D’Alambert’s principle, the governing equations of motion can be written as follow:

$$\begin{aligned} -f_{s1} - f_{d1} + f_{s2} + f_{d2} &= m_1 \ddot{x}_1 \\ -k_1(x_1 - x_0) - c_1(\dot{x}_1 - \dot{x}_0) + k_2(x_2 - x_1) + c_2(\dot{x}_2 - \dot{x}_1) &= m_1 \ddot{x}_1 \\ m_1 \ddot{x}_1 + (c_1 + c_2)\dot{x}_1 - c_2\dot{x}_2 + (k_1 + k_2)x_1 - k_2x_2 &= 0 \\ \\ -f_{s2} - f_{d2} + f_{s3} + f_{d3} &= m_2 \ddot{x}_2 \\ -k_2(x_2 - x_1) - c_2(\dot{x}_2 - \dot{x}_1) + k_3(x_3 - x_2) + c_3(\dot{x}_3 - \dot{x}_2) &= m_2 \ddot{x}_2 \\ m_2 \ddot{x}_2 - c_2\dot{x}_1 + (c_2 + c_3)\dot{x}_2 - c_3\dot{x}_3 - k_2x_1 + (k_2 + k_3)x_2 - k_3x_3 &= 0 \\ \\ -f_{s3} - f_{d3} + f_{sd} + f_{dd} &= m_3 \ddot{x}_3 \\ -k_3(x_3 - x_2) - c_3(\dot{x}_3 - \dot{x}_2) + k_d(x_d - x_3) + c_d(\dot{x}_d - \dot{x}_3) &= m_3 \ddot{x}_3 \\ m_3 \ddot{x}_3 - c_3\dot{x}_2 + (c_3 + c_d)\dot{x}_3 - c_d\dot{x}_d - k_2x_2 + (k_3 + k_d)x_3 - k_dx_d &= 0 \\ \\ -f_{sd} - f_{dd} &= m_d \ddot{x}_d \\ -k_d(x_d - x_3) - c_d(\dot{x}_d - \dot{x}_3) &= m_d \ddot{x}_d \end{aligned}$$

$$m_d \ddot{x}_d - c_d \dot{x}_3 + c_d \dot{x}_d - k_d x_3 + k_d x_d = 0$$

$$[M]\{\ddot{x}(t)\} + [C]\{\dot{x}(t)\} + [K]\{x(t)\} = \{\delta\}\ddot{x}_a(t)$$

Where the mass matrix M formed as a diagonal lumped mass matrix of $100 \times 10^3 \text{ kg}$ for each floor and assumed to be rigid in their own plane owing to the diaphragm action of the floor slab. The total stiffness matrix is formed of $k_1 = 41 \times 10^6 \text{ N/m}$, $k_2 = 38 \times 10^6 \text{ N/m}$, and $k_3 = 36 \times 10^6 \text{ N/m}$ by assembling all the elements in symmetrical order where the columns and beams are inextensible and weightless. The damping matrix is then determined as a proportional damping.

$$[M] = \begin{bmatrix} m_1 & 0 & 0 & 0 \\ 0 & m_2 & 0 & 0 \\ 0 & 0 & m_3 & 0 \\ 0 & 0 & 0 & m_d \end{bmatrix} = \text{Mass Matrix}$$

$$\ddot{x}(t) = \begin{bmatrix} \ddot{x}_1 \\ \ddot{x}_2 \\ \ddot{x}_3 \\ \ddot{x}_d \end{bmatrix} = \text{Acceleration Matrix}$$

$$[C] = \begin{bmatrix} c_1 + c_2 & -c_2 & 0 & 0 \\ -c_2 & c_2 + c_3 & -c_3 & 0 \\ 0 & -c_3 & c_3 + c_d & -c_d \\ 0 & 0 & -c_d & c_d \end{bmatrix} = \text{Damping Matrix,}$$

$$\dot{x}(t) = \begin{bmatrix} \dot{x}_1 \\ \dot{x}_2 \\ \dot{x}_3 \\ \dot{x}_d \end{bmatrix} = \text{Velocity Matrix}$$

$$[K] = \begin{bmatrix} k_1 + k_2 & -k_2 & 0 & 0 \\ -k_2 & k_2 + k_3 & -k_3 & 0 \\ 0 & -k_3 & k_3 + k_d & -k_d \\ 0 & 0 & -k_d & k_d \end{bmatrix} = \text{Stiffness Matrix,}$$

$$x(t) = \begin{bmatrix} x_1 \\ x_2 \\ x_3 \\ x_d \end{bmatrix} = \text{Displacement Matrix}$$

The TMD location is also rearranged according to the other two dominant structural modes which the effects of structural rotation in this study is neglected. For the purpose of the analysis, the primary structure is assumed remain intact within elastic limit during earthquake where the ground motion component is unidirectional with the soil structure interaction is neglected. *Table 1* shows the summary of primary structure-TMD parameters.

Table 1: Summary of Primary Structure-TMD Parameters

| PARAMETER | SYMBOL | TMD 1 | TMD 2 | TMD 3 |
|--|---------------|------------|------------|------------|
| Generalized Modal Stiffness (N/m) | $k_{n\ mode}$ | 1.3931E+07 | 1.1626E+08 | 2.3768E+08 |
| Generalized Modal Mass (kg) | $m_{n\ mode}$ | 178910 | 197450 | 194280 |
| Damper Mass (kg) | m_d | 15000 | 15000 | 15000 |
| Mass Ratio | μ | 0.08 | 0.08 | 0.08 |
| Primary Structure Damping Ratio | ξ_{ps} | 0.0499 | 0.0697 | 0.0928 |
| Optimum Damping Ratio | ξ_{opt} | 0.2210 | 0.2231 | 0.2372 |
| Modal Damping Ratio | ξ_{md} | 0.1355 | 0.1464 | 0.1650 |
| Damping Efficiency | η | 0.6316 | 0.5238 | 0.4376 |
| Generalized Mass Ratio | μ_{gen} | 0.08 | 0.08 | 0.08 |
| Optimum Frequency Ratio | f_{opt} | 0.9023 | 0.9005 | 0.8875 |
| Optimum TMD Stiffness (N/m) | $k_{d\ opt}$ | 950897 | 7161917 | 14452629 |
| Optimum TMD Damping Coefficient (Ns/m) | $c_{d\ opt}$ | 52795 | 146215 | 220902 |

3.2 Design of TMD for Multiple Degree of Freedom Structure

A common TMD consists of few elements such as mass, spring, and dashpot attached to a primary structure purposely to attenuate its dynamic response. Fundamentally, the frequency of TMD is tuned particularly to the main structure so that it will resonates out of phase during excitation and dissipating the input energy force which acting to the structure. In the case of multiple degree of freedom structure, the designation of the TMD need to be focused on a

specific target vibration mode. In order to simplify a multiple degree of freedom system into a generalized two degree of freedom model, proposed a generalized stiffness and generalized mass a corresponding target mode.

$$k_{n\ modes} = \frac{\varphi_t^T K \varphi_t}{(w^T \varphi_t)^2}$$

$$m_{n\ modes} = \frac{\varphi_t^T M \varphi_t}{(w^T \varphi_t)^2}$$

Where K and M are stiffness and mass matrices of the primary structure and $\varphi_t / (w^T \varphi_t)$ is the normalized mode shape of target mode. The index vector w is an element unit of the TMD placement upon the primary structure. Has proposed design procedure for TMD for multiple degree of freedom structure by defining damping efficiency (η) as the resonance amplification factor of TMD-structure system as follow

$$\eta = 1 - \frac{\xi_{ps}}{\xi_{md}}$$

Where modal damping ratio (ξ_{md}) can be expressed as

$$\xi_{md} = \frac{1}{2}(\xi_{ps} + \xi_{opt})$$

and the optimal damping ratio ξ_{opt} corresponding to the dynamic amplification extremum value is taken as the following form

$$\xi_{opt} = \frac{\xi_{ps} + \sqrt{\xi_{ps}^2 + 2\mu(1 + \mu)}}{2(1 + \mu)}$$

Then the generalized mass ratio (μ_{gen}) can be determined by the corresponding target damping efficiency

$$\mu_{gen} = \frac{4\eta(1+\eta)\xi_{ps}^2}{(1-\eta)^2 - 2(1+\eta)^2\xi_{ps}^2}$$

For the determination of an optimal frequency ratio, the μ_{gen} is taking part in the following equation

$$f_{opt} = \frac{1}{1 + \mu_{gen}\xi_2 / (\xi_{opt} - \xi_{ps})}$$

Consequently, the optimum stiffness and damping coefficient of the designed TMD can be written as follow

$$k_{d\ opt} = f_{opt}^2 \mu_{gen} k_{n\ mode}$$

$$c_{d\ opt} = 2f_{opt}\mu \sqrt{k_{n\ mode} m_{n\ mode} \xi_{opt}}$$

Table 2 to Table 5 summarized structural parameters that represent various vibration control arrangements. The MTMD1 is depicted the TMDs are located at the third and first floor, MTMD2 where the TMDs located at second and first floor, MTMD3 where the TMDs located at the third and second floor, and MTMD4 defined that TMDs located at all primary structural floors. The variation of structural parameters differ among the different kind of TMD arrangements are directly proportionated to the justifications of generalized modal stiffness and generalized modal mass which initially obtained from dynamic response analysis of primary structure using Newmark's time stepping method. Within the study, the effect of implementing base isolation system is also considered for all TMD mechanisms. The horizontal stiffness of the isolation bearing is determined by considering that rubber compound damping ratio is 0.15 and

the target period for the designated bearing is 2.5 second. Therefore, both horizontal stiffness and damping coefficient of an isolation bearing is 3,158,273 N/m and 471,239 Ns/m.

Table 2: Summary of Primary Structure-MTMD1 Parameters

| PARAMETER | SYMBOL | MTMD1 | |
|--|---------------|----------------------|----------------------|
| | | TMD 1 (3rd Floor) | TMD 2 (1st Floor) |
| Generalized Modal Stiffness (N/m) | $k_{n\ mode}$ | 6.9266E+06 | 4.1763E+09 |
| Generalized Modal Mass (kg) | $m_{n\ mode}$ | 88952 | 7093000 |
| Damper Mass (kg) | m_d | 5000 | 10000 |
| Mass Ratio | μ | 0.06 | 0.00 |
| Primary Structure Damping Ratio | ξ_{ps} | 0.0499 | 0.0697 |
| Optimum Damping Ratio | ξ_{opt} | 0.1884 | 0.0786 |
| Modal Damping Ratio | ξ_{md} | 0.1192 | 0.0741 |
| Damping Efficiency | η | 0.5813 | 0.0598 |
| Generalized Mass Ratio | μ_{gen} | 0.06 | 0.001 |
| Optimum Frequency Ratio | f_{opt} | 0.9290 | 0.9877 |
| Optimum TMD Stiffness (N/m) | $k_{d\ opt}$ | 336003 | 5743454 |
| Optimum TMD Damping Coefficient (Ns/m) | $c_{d\ opt}$ | 15448 | 37656 |

Table 3: Summary of Primary Structure-MTMD2 Parameters

| PARAMETER | SYMBOL | MTMD2 | |
|--|---------------|----------------------|----------------------|
| | | TMD 3 (2nd Floor) | TMD 2 (1st Floor) |
| Generalized Modal Stiffness (N/m) | $k_{n\ mode}$ | 1.5687E+10 | 4.9696E+07 |
| Generalized Modal Mass (kg) | $m_{n\ mode}$ | 12823000 | 84404 |
| Damper Mass (kg) | m_d | 5000 | 10000 |
| Mass Ratio | μ | 0.00 | 0.12 |
| Primary Structure Damping Ratio | ξ_{ps} | 0.0928 | 0.0697 |
| Optimum Damping Ratio | ξ_{opt} | 0.0948 | 0.2634 |
| Modal Damping Ratio | ξ_{md} | 0.0938 | 0.1665 |
| Damping Efficiency | η | 0.0108 | 0.5815 |
| Generalized Mass Ratio | μ_{gen} | 0.0004 | 0.12 |
| Optimum Frequency Ratio | f_{opt} | 0.9820 | 0.8612 |
| Optimum TMD Stiffness (N/m) | $k_{d\ opt}$ | 5898746 | 4367280 |
| Optimum TMD Damping Coefficient (Ns/m) | $c_{d\ opt}$ | 32568 | 110090 |

Table 4: Summary of Primary Structure-MTMD3 Parameters

| PARAMETER | SYMBOL | MTMD3 | |
|--|---------------|----------------------|----------------------|
| | | TMD 1 (3rd Floor) | TMD 3 (2nd Floor) |
| Generalized Modal Stiffness (N/m) | $k_{n\ mode}$ | 4.3787E+06 | 6.9924E+08 |
| Generalized Modal Mass (kg) | $m_{n\ mode}$ | 56232 | 571580 |
| Damper Mass (kg) | m_d | 5000 | 10000 |
| Mass Ratio | μ | 0.09 | 0.02 |
| Primary Structure Damping Ratio | ξ_{ps} | 0.0499 | 0.0928 |
| Optimum Damping Ratio | ξ_{opt} | 0.2263 | 0.1489 |
| Modal Damping Ratio | ξ_{md} | 0.1381 | 0.1209 |
| Damping Efficiency | η | 0.6386 | 0.2322 |
| Generalized Mass Ratio | μ_{gen} | 0.09 | 0.02 |
| Optimum Frequency Ratio | f_{opt} | 0.8976 | 0.9556 |
| Optimum TMD Stiffness (N/m) | $k_{d\ opt}$ | 313692 | 11172159 |
| Optimum TMD Damping Coefficient (Ns/m) | $c_{d\ opt}$ | 17922 | 99560 |

Table 5: Summary of Primary Structure-MTMD4 Parameters

| PARAMETER | SYMBOL | MTMD4 | | |
|--|---------------|----------------------|----------------------|---------------------|
| | | TMD 1 (3rd Floor) | TMD 2 (1st Floor) | TMD3 (2nd Floor) |
| Generalized Modal Stiffness (N/m) | $k_{n\ mode}$ | 2.8734E+06 | 2.3976E+08 | 2.7517E+09 |
| Generalized Modal Mass (kg) | $m_{n\ mode}$ | 36901 | 407210 | 2249300 |
| Damper Mass (kg) | m_d | 5000 | 5000 | 5000 |
| Mass Ratio | μ | 0.1355 | 0.0123 | 0.0022 |
| Primary Structure Damping Ratio | ξ_{ps} | 0.0499 | 0.0697 | 0.0928 |
| Optimum Damping Ratio | ξ_{opt} | 0.2672 | 0.1196 | 0.1033 |
| Modal Damping Ratio | ξ_{md} | 0.1586 | 0.0946 | 0.0981 |
| Damping Efficiency | η | 0.6853 | 0.2635 | 0.0537 |
| Generalized Mass Ratio | μ_{gen} | 0.1355 | 0.0123 | 0.0022 |
| Optimum Frequency Ratio | f_{opt} | 0.8572 | 0.9714 | 0.9786 |
| Optimum TMD Stiffness (N/m) | $k_{d\ opt}$ | 286073 | 2777972 | 5858358 |
| Optimum TMD Damping Coefficient (Ns/m) | $c_{d\ opt}$ | 20213 | 28185 | 35369 |

3.3 Formulation of State Space Equation

In order to form state representation of structure-TMD mechanism, equation can be rearranged as follow

$$\{\ddot{x}(t)\} = -[M]^{-1}[C]\{\dot{x}(t)\} - [M]^{-1}[K]\{x(t)\} + [M]^{-1}\{\delta\}\ddot{x}_g(t)$$

Where,

$$\{\dot{x}(t)\} = [I]\{x(t)\}$$

An equation can be expressed as follow

$$\begin{Bmatrix} \{\dot{x}(t)\} \\ \{\ddot{x}(t)\} \end{Bmatrix} = \begin{bmatrix} [0] & [I] \\ -[M]^{-1}[K] & -[M]^{-1}[C] \end{bmatrix} \begin{Bmatrix} \{x(t)\} \\ \{\dot{x}(t)\} \end{Bmatrix} + \begin{Bmatrix} \{0\} \\ [M]^{-1}\{\delta\} \end{Bmatrix} \ddot{x}_g(t)$$

The second order motion of equation is cast into its first order representation by defining the following state vector

$$\{Z(t)\} = \begin{Bmatrix} \{x(t)\} \\ \{\dot{x}(t)\} \end{Bmatrix}$$

Then equation can be rewritten into state form as

$$\{\dot{Z}(t)\} = [A]\{Z(t)\} + \{B_r\}\ddot{x}_g(t)$$

$$\{Y\} = [E_0]\{Z(t)\}$$

Where

$$\{\dot{Z}(t)\} = \begin{Bmatrix} \{\dot{x}(t)\} \\ \{\ddot{x}(t)\} \end{Bmatrix}_{2n \times 1}$$

Where

$$[A] = \begin{bmatrix} [0] & [I] \\ -[M]^{-1}[K] & -[M]^{-1}[C] \end{bmatrix}_{2n \times 2n}$$

$$\{B_r\} = \begin{Bmatrix} \{0\} \\ [M]^{-1}\{\delta\} \end{Bmatrix}_{2n \times 1}$$

E_0 =Measurement Matrix

Figure 1 below show the Simulink diagram of state space solution for multiple degree of freedom system. The output of the solutions are displacement, velocity and acceleration sampled at the given time interval.

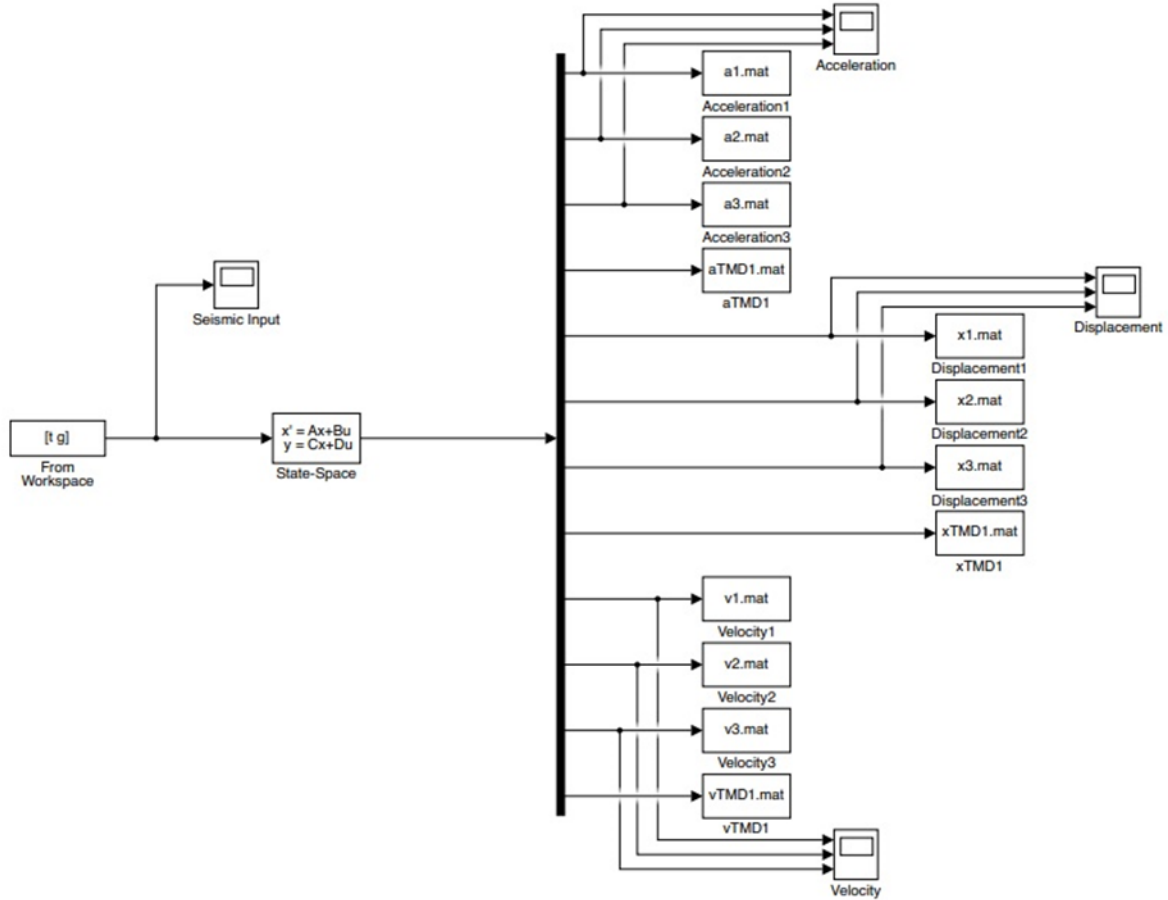
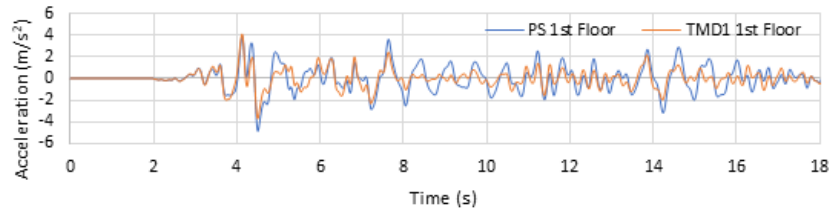


Figure 1: Simulink Diagram for State Space Solution for Multiple Degree of Freedom System

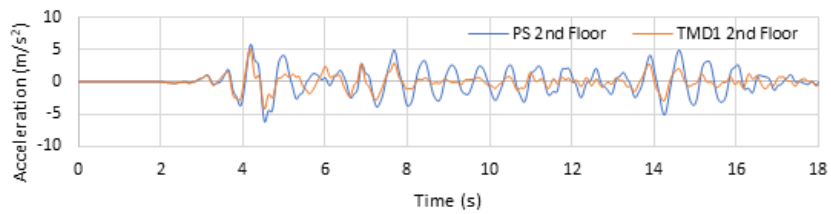
4. Results and Discussion

The analytical investigation of structural responses was conducted using MATLAB by considering the parameters for various arrangement of both single and multiple TMD. The primary structure was subjected to the El-Centro 1940 earthquake. Within the analysis, the performance between single and multiple TMD is compared towards uncontrolled primary structure in terms of reducing floors acceleration. *Figure 2* and *Figure 3* shows the time history of structural accelerations and displacements responses for single TMD located at the different floor which in general, the maximum structural responses are reduced. It can be observed that the placement of TMD at the top floor (TMD1) which contributed to the largest amplitude corresponding to vibration mode shapes reduced peak acceleration of uncontrolled structure from

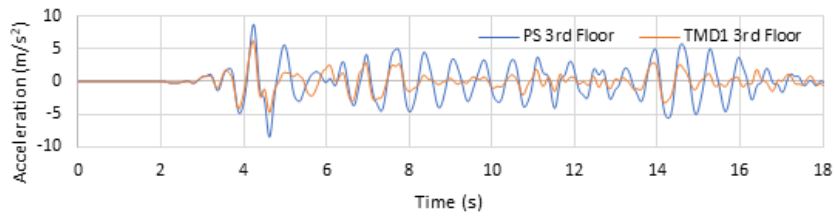
8.48 m/s² to 5.75 m/s². Similarly, as the main concern is to limit the vibration of the top floor, the maximum displacement is also reduced from 0.09 m to 0.04 m.



(a)



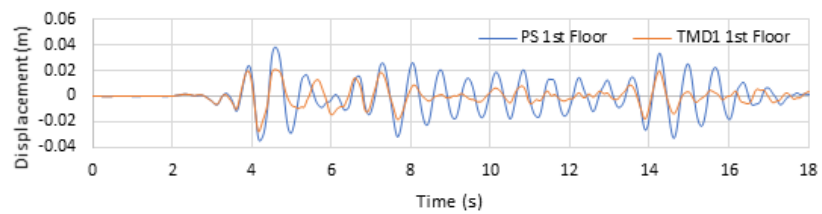
(b)



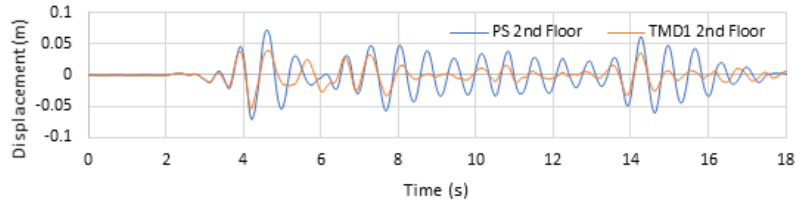
(c)

Figure 2: Structural Acceleration Responses of Time History Analysis for TMD1

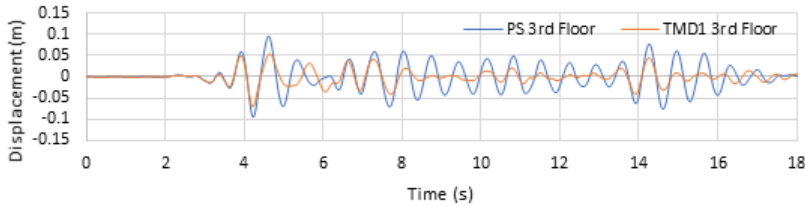
(a) First Floor (b) Second Floor (c) Third Floor



(a)



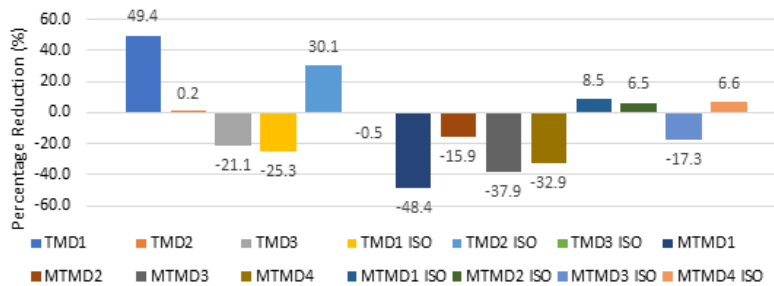
(b)



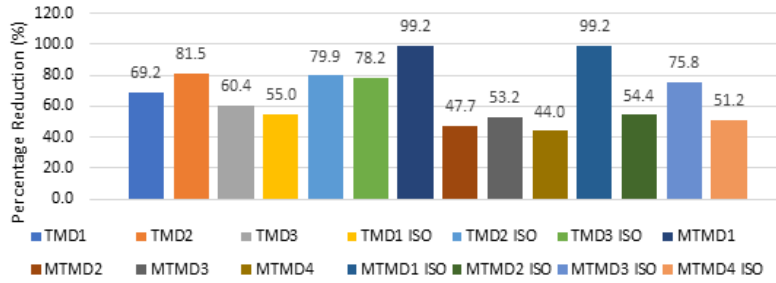
(c)

Figure 3: Structural Displacement Responses of Time History Analysis for TMD1
 (a) First Floor (b) Second Floor (c) Third Floor

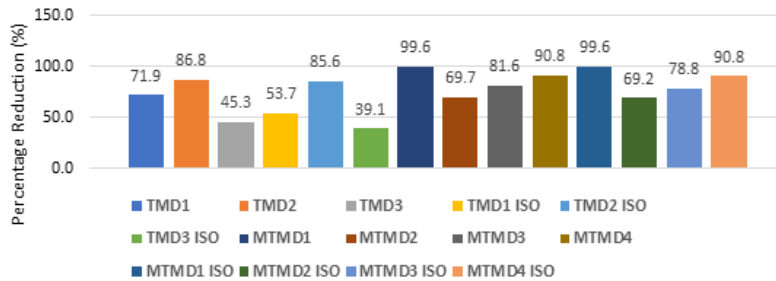
In order to improve the efficiency of different TMD arrangement, Root Mean Square (RMS) value structural responses are evaluated in this study. *Figure 4* show the percentage reduction of RMS acceleration for various TMD arrangements compared to the uncontrolled primary structure for each of structural floors. From the obtained results, it is observed that only TMD1, TMD2 ISO, MTMD1 ISO, MTMD2 ISO, and MTMD4 ISO contributed to the reduction of first floor vibration which the highest percentage represented by TMD1 with 49.4%. However, significant percentage reduction of structural RMS acceleration discovered for all TMD arrangement for both second and third structural floor which the highest percentage conferred by TMD1 ISO and MTMD1 ISO with 99.2%. It can be justified that the base isolation system is capable for further lessen the dedicated structural floor for both TMD and MTMD system.



(a)



(b)

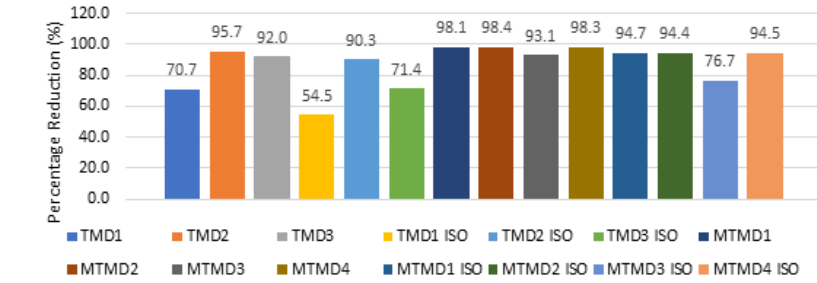


(c)

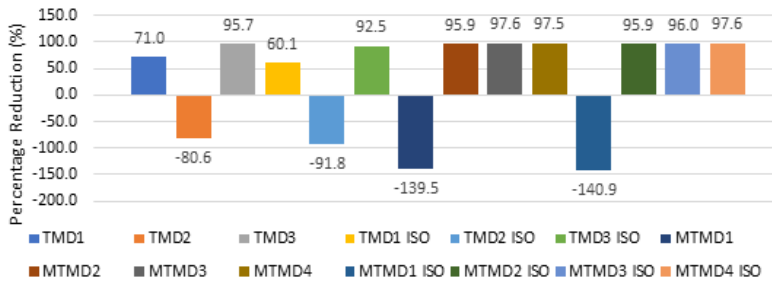
Figure 4: Structural RMS Acceleration Percentage Reduction of Various TMD arrangement

(a) First Floor (b) Second Floor (c) Third Floor

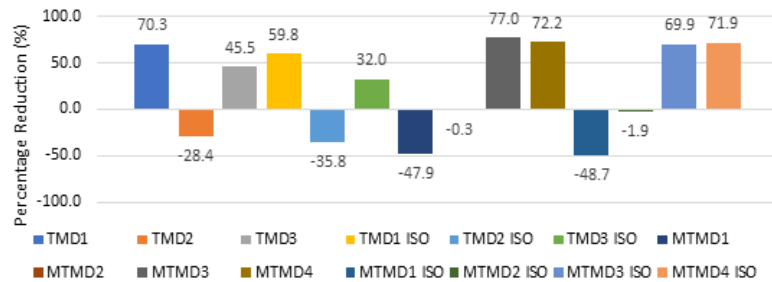
Purposely to broaden the investigation on the proposed structural control system, the observation on the structural displacement is also taken into account. *Figure 5* shows corresponding data on the percentage reduction of RMS displacement compare to the uncontrolled primary structure. From the chart, it can be stated that each of the proposed TMD arrangement contributed to a promising result in terms of controlling the first-floor displacement which the highest percentage recorded by MTMD4 with 98.4% reduction. Despite that, TMD arrangement such as TMD2, TMD2 ISO, MTMD1, and MTMD1 ISO did not come up with a convincing result to decrease displacement of second and third structural floor. Nevertheless, the rest of passive control system is able to significantly manifest the effectiveness of controlling both second and third floor which MTMD3 and MTMD4 ISO produced the highest percentage reduction of 97.6% while for the third floor goes to MTMD3 with 77%.



(a)



(b)

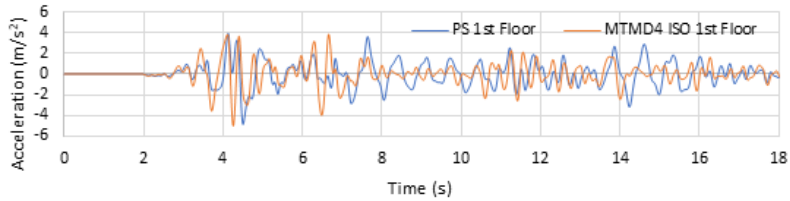


(c)

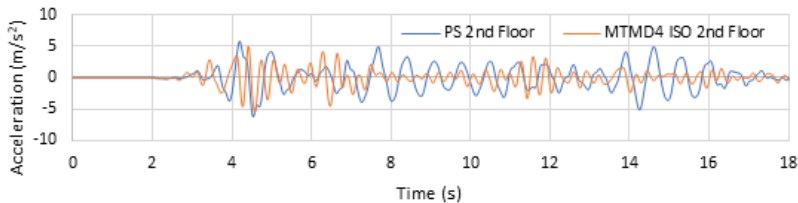
Figure 5: Structural RMS Displacement Percentage Reduction of Various TMD arrangement
(a) First Floor (b) Second Floor (c) Third Floor

Among the overall proposed TMD control system, MTMD4 ISO demonstrated encouraging performance in both acceleration & displacement perspectives. This matter is proven as the arrangement achieved the main objective of controlling top floor structural drift and displacement while at the same time influence the capability of reducing responses of others primary structural floors. *Figure 6* show the structural acceleration responses of primary structure with and without the MTMD4 ISO mechanism. The uncontrolled primary structure floors RMS acceleration are stated as 0.7266 m/s^2 for the first floor, 1.8848 m/s^2 for the second floor, and 3.1476 m/s^2 . Comparing the data towards the controlled manner of MTMD4 ISO which the RMS drift for the

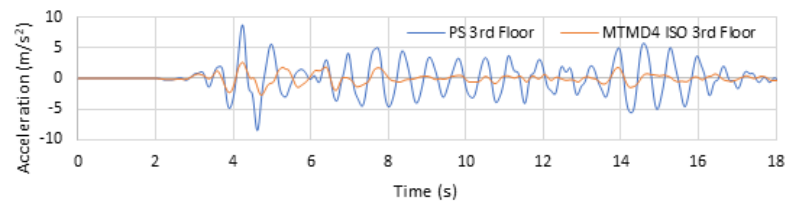
first and second floors which are 0.6787 m/s^2 and 0.9196 m/s^2 , the reduction is considered acceptable since the top floor performed really well to decreased the RMS acceleration to 0.2905 m/s^2 . On the other hand, MTMD4 ISO performed well in terms of reducing RMS displacement for all structural floors especially in between 0 to 18 seconds of vibration time history. Within the time range, it can be observed that the MTMD4 ISO implementation not only reduced the RMS displacement but also able to outstandingly counter the peak structural displacement.



(a)



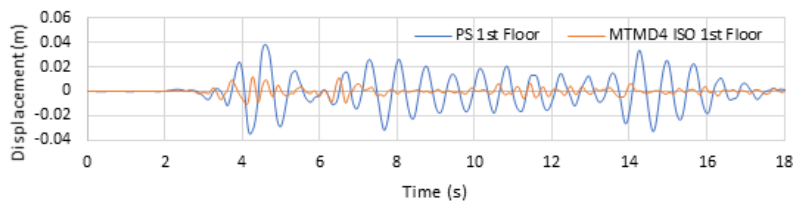
(b)



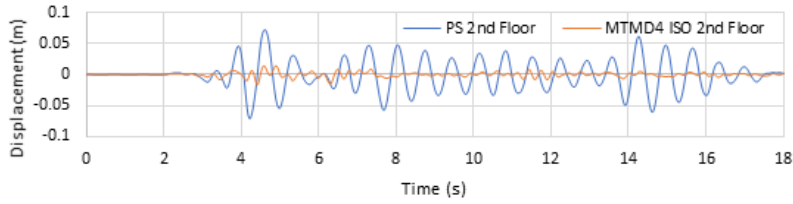
(c)

Figure 6: Structural Acceleration Responses of Time History Analysis for MTMD4 ISO

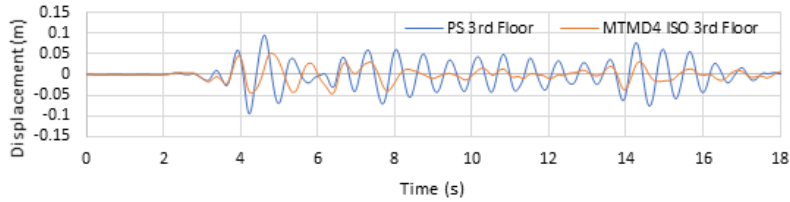
(a) First Floor (b) Second Floor (c) Third Floor



(a)



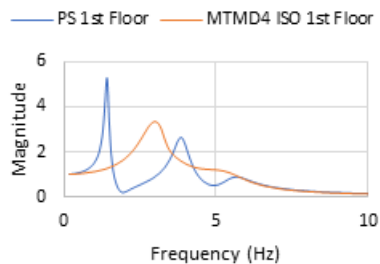
(b)



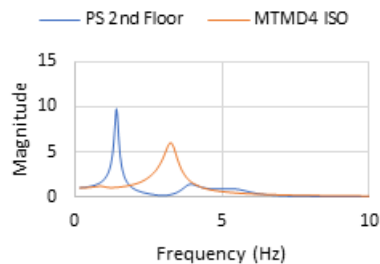
(c)

Figure 7: Structural Displacement Responses of Time History Analysis for MTMD4 ISO
 (a) First Floor (b) Second Floor (c) Third Floor

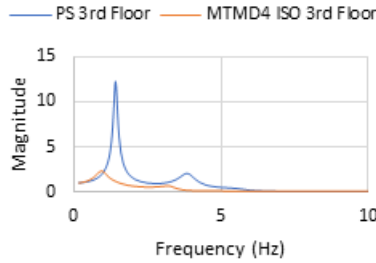
Figure 8 depicted the plots of dynamic amplification factor as a function of seismic excitation input normalized by the uncontrolled primary structure natural frequency. From the graph, it can be observed that the frequency response function curves of MTMD4 ISO acquired two unequal local maxima for both second and third primary structural floor. However, for the case of third floor, the local maxima are almost equal and much lower comparing to the uncontrolled case. This comparison is meaningful to prove that the MTMD4 ISO arrangement capable of reducing significant amount of primary structure top floor peak dynamic amplification while at the same time reliable of controlling the other two floors.



(a)



(b)

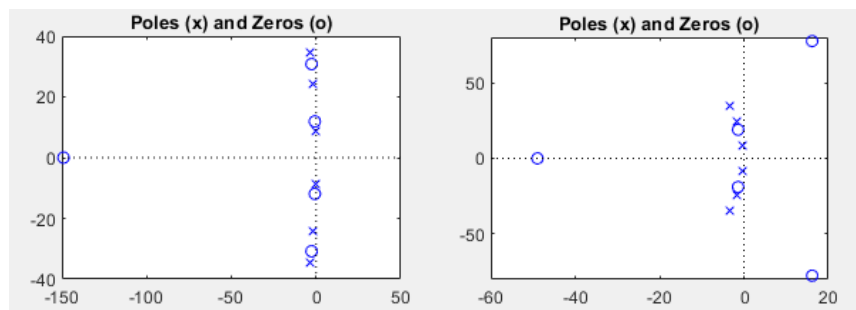


(c)

Figure 8: Dynamic Amplification Factor of PS-MTMD4 ISO

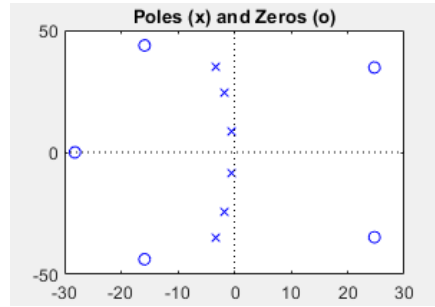
(a) First Floor (b) Second Floor (c) Third Floor

Vibration control system can also be characterized by observing system poles and zeros in the sense of reconstruction of system differential equation. Conceptually, the poles and zeros of a system transfer function to define a dynamic system in graphical plot manner on the complex s -plane. The poles and zero location are able to provide a qualitative determination of vibration system characteristics. *Figure 9* and *Figure 10* shows poles and zeros diagram for both uncontrolled primary structure and MTMD4 ISO system. The vertical axis is considered as imaginary axis while on the horizontal axis is real axis. From the figures, the poles (the x symbol) state is in pair complex conjugate located at the left half of the s -plane. It means that all the systems responses decaying in sinusoidal form. Fundamentally, poles far from origin of the left half of s -plane real-axis correspond to rapid decay while poles near the origin will response in a slow manner over the time. From the figures, it can be concluded that the poles for the PS-MTMD4 ISO is located near to the real-axis of the left half s -plane which considered the system improved the primary structural responses to decay more rapid than the uncontrolled primary structure.



(a)

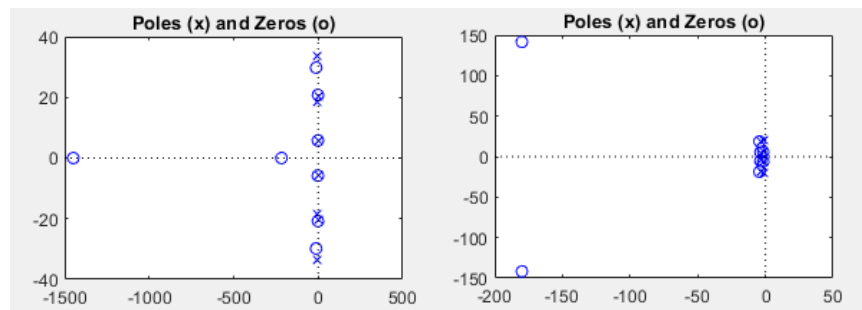
(b)



(c)

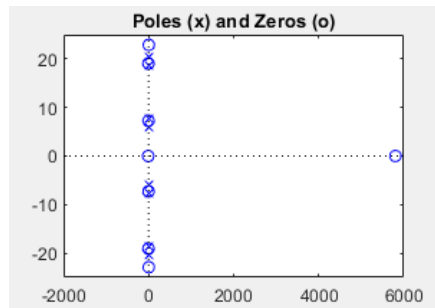
Figure 9: Poles and Zero Diagram of PS

(a) First Floor (b) Second Floor (c) Third Floor



(a)

(b)



(c)

Figure 10: Poles & Zero Diagram of PS-MTMD4 ISO

(a) First Floor (b) Second Floor (c) Third Floor

5. Conclusion

The seismic structural responses of a 3-story structure are analyzed by implementing various TMD mechanism arrangement. The main objective of this study is to evaluate the capability of the various proposal of TMD mechanism to control structural acceleration and displacement. By comparing all the structural control mechanism, MTMD4 ISO is identified as the most reliable mechanism in terms of minimizing RMS & peak responses of all structural

floors with a significant reduction. The following conclusion are drawn to represent the result obtained from the study:

1. The installation of MTMD is significantly capable of reducing structural acceleration responses of both second and third floor.
2. The designated base isolation system is promising on the improvement both TMD and MTMD efficiency to control floors vibrations.
3. The top floor TMD is a must in order to control large structural displacement of the first structural mode.
4. The MTMD mechanism equipped with base isolation system is more effective compare to single TMD and MTMD without base isolation system in terms of reducing both structural acceleration and displacement of all floors.

References

- [1] T. E. Saaed, G. Nikolakopoulos, J.-E. Jonasson, and H. Hedlund, "A state-of-the-art review of structural control systems," *J. Vib. Control*, vol. 21, no. 5, pp. 919–937, 2015, doi: 10.1177/1077546313478294.
- [2] L. K. Cheng F.Y., Jiang H., *Smart Structures Innovative Systems for Seismic Response Control*. 2008.
- [3] B. Zhao, H. Gao, Z. Wang, and Z. Lu, "Shaking table test on vibration control effects of a monopile offshore wind turbine with a tuned mass damper," *Wind Energy*, vol. 21, no. 12, pp. 1309–1328, 2018, doi: 10.1002/we.2256.
- [4] S. Y. Kim and C. H. Lee, "Optimum design of linear multiple tuned mass dampers subjected to white-noise base acceleration considering practical configurations," *Eng. Struct.*, vol. 171, no. May, pp. 516–528, 2018, doi: 10.1016/j.engstruct.2018.06.002.
- [5] H. Anajafi and R. A. Medina, "Comparison of the seismic performance of a partial mass isolation technique with conventional TMD and base-isolation systems under broad-band and narrow-band excitations," *Eng. Struct.*, vol. 158, no. December 2017, pp. 110–123, 2018, doi: 10.1016/j.engstruct.2017.12.018.
- [6] P. Brzeski, M. Lazarek, and P. Perlikowski, "Experimental study of the novel tuned mass damper with inerter which enables changes of inertance," *J. Sound Vib.*, 2017, doi: 10.1016/j.jsv.2017.05.034.
- [7] P. Tan, C. J. Fang, C. M. Chang, B. F. Spencer, and F. L. Zhou, "Dynamic characteristics of novel energy dissipation systems with damped outriggers," *Eng. Struct.*, vol. 98, pp. 128–140, 2015, doi: 10.1016/j.engstruct.2015.04.033.
- [8] S. Nagarajaiah and E. Sonmez, "Structures with Semiactive Variable Stiffness Single/Multiple Tuned Mass Dampers," *J. Struct. Eng.*, vol. 133, no. 1, pp. 67–77, 2007, doi: 10.1061/(ASCE)0733-9445(2007)133:1(67).
- [9] A. Javanmardi, Z. Ibrahim, K. Ghaedi, H. Benisi Ghadim, and M. U. Hanif, "State-of-the-Art Review of Metallic Dampers: Testing, Development and Implementation," *Arch.*

- Comput. Methods Eng.*, no. March, 2019, doi: 10.1007/s11831-019-09329-9.
- [10] M. Gu, S. R. Chen, and C. C. Chang, “Parametric study on multiple tuned mass dampers for buffeting control of Yangpu Bridge,” *J. Wind Eng. Ind. Aerodyn.*, vol. 89, no. 11–12, pp. 987–1000, 2001, doi: 10.1016/S0167-6105(01)00094-0.
- [11] Y. Daniel and O. Lavan, “Optimality criteria based seismic design of multiple tuned-mass-dampers for the control of 3D irregular buildings,” *Earthq. Struct.*, vol. 8, no. 1, pp. 77–100, 2015, doi: 10.12989/eas.2015.8.1.077.
- [12] B. Mokrani, Z. Tian, D. Alaluf, F. Meng, and A. Preumont, “Passive damping of suspension bridges using multi-degree of freedom tuned mass dampers,” *Eng. Struct.*, vol. 153, no. December, pp. 749–756, 2017, doi: 10.1016/j.engstruct.2017.10.028.
- [13] S. M. Nigdeli and G. Bekdaş, “Optimum tuned mass damper design in frequency domain for structures,” *KSCE J. Civ. Eng.*, vol. 21, no. 3, pp. 912–922, 2017, doi: 10.1007/s12205-016-0829-2.
- [14] Z. Shu, S. Li, X. Sun, and M. He, “Performance-based Seismic Design of a Pendulum Tuned Mass Damper System,” *J. Earthq. Eng.*, vol. 23, no. 2, pp. 334–355, 2019, doi: 10.1080/13632469.2017.1323042.
- [15] H. Fang, L. Liu, D. Zhang, and M. Wen, “Tuned mass damper on a damped structure,” *Struct. Control Heal. Monit.*, vol. 26, no. 3, pp. 1–16, 2019, doi: 10.1002/stc.2324.